ELSEVIER

Composite Structures 46 (1999) 103–113

COMPOSITE STRUCTURES

Partial-mixed formulation and refined models for the analysis of composite laminates within an FSDT

Ferdinando Auricchio [a], Elio Sacco [b,*]

[a] *Dipartimento di Ingegneria Civile, Università di Roma "Tor Vergata", Via di Tor Vergata, 00133 Roma, Italy*
[b] *Dipartimento di Ingegneria Industriale, Università di Cassino, Via Di Biasio 43, 03043 Cassino, Italy*

Abstract

The present paper proposes a partial-mixed variational formulation for the analysis of composite laminates within the First-order Shear Deformation Theory (FSDT). The considered functional is recovered from the Hellinger–Reissner mixed principle and it appears to be particularly suitable for the determination of the FSDT governing equations since the transverse shear stresses are treated as independent variables. Accordingly, it is possible to obtain an accurate description of the shear stress profiles. Herein, the attention is concentrated on two different refined FSDT models, both having piecewise parabolic shear stress profiles. Furthermore, within one of the two refined models, the partial-mixed formulation is used to derive a performing finite element. Finally, analytical solutions from the classical and the refined FSDT models are compared to three-dimensional (3D) analytical solutions as well as to results obtained form the proposed laminate finite element.

Keywords: Composite laminates; First-order Shear Deformation Theory (FSDT); Partial-mixed formulation

1. Introduction

Laminate theories reduce the study of a three-dimensional (3D) layered body to a two-dimensional (2D) problem. This 3D–2D reduction is in general performed assuming specific laminate structural behaviors, i.e. introducing hypotheses on the strain field or on the stress field or on both the strain and the stress fields. According to these different possibilities, several laminate models have been proposed in the literature [1,2].

In general, laminate theories based on both strain and stress hypotheses lead to models characterized by good performances. Within this approach, the most used formulation is the so-called First-order Shear Deformation Theory (FSDT). Originally developed by Yang et al. [3] and by Whitney and Pagano [4] as an extension of the plate theory proposed by Reissner [5] and Mindlin [6], the FSDT allows the determination of accurate solutions for a wide class of laminate problems.

Although the most common FSDT variational formulations are based on displacement approaches, mixed formulations have been proposed in the literature, mainly for the definition of innovative finite elements, e.g. see Refs. [7–10].

However, it is fundamental to observe that the correct use of the FSDT requires the definition of through-the-thickness shear stress profiles, leading to the determination of the so-called shear correction factors. Unfortunately, these profiles are known a priori only for homogeneous plates or for cross-ply laminates under cylindrical bending and not for general lamination sequences [11–13]; this aspect represents a clear limitation to a correct use of the FSDT.

To overcome this difficulty, two different approaches can be found in the literature. The first approach is based on the refinement of the model by the use of additive shear warping functions, e.g. see Refs. [14,15], leading to an increment in the kinematic unknowns. This refinement clearly makes the method more expensive from a computational viewpoint. The second approach consists in the development of iterative procedures, as the one proposed by Noor and coworkers and based on the analytical solution of rectangular laminates subjected to sinusoidal loading [16–18]. However, these iterative procedures are not extendable to generic laminates geometries.

The present work starts with a review of the FSDT together with a detailed discussion of the basic hypotheses introduced to construct the model. Then, from the Hellinger–Reissner functional, a partial-mixed functional for the FSDT is recovered. The obtained

* Corresponding author. E-mail: sacco@ing.unicas.it

0263-8223/99/$ – see front matter
PII: S0263-8223(99)00035-5

formulation is used to derive two refined laminate models based on the classical FSDT kinematics and on the definition of suitable shear stress profiles in the laminate thickness.

The first refined model (RM1-FSDT) is based on the use of specific shear stress profiles directly in the proposed partial-mixed variational functional.

The second refined model (RM2-FSDT) is based on an iterative predictor–corrector procedure for the determination of the laminate response. The iterative procedure is rationally derived using the presented partial-mixed formulation, and recovers the analytical approach proposed in Refs. [16–18] for the case of rectangular laminates subjected to sinusoidal loading. Furthermore, the variational formulation adopted allows the development of a robust laminate finite element (EML4) for this model.

Solutions from the classical and the refined FSDT models are compared to 3D analytical solutions for different lamination sequences.

2. First-order laminate theory (FSDT)

A laminate plate Ω refers to a flat body, with constant thickness $2h$:

$$\Omega = \left\{(x_1, x_2, z) \in \mathbb{R}^3 / z \in (-h, h),\ (x_1, x_2) \in \mathscr{A} \subset \mathbb{R}^2\right\}, \tag{1}$$

where the plane $z = 0$ identifies the mid-plane $\mathscr{A}$ of the undeformed plate. The laminate is made of n layers and the typical kth layer lies between the thickness coordinates z_{k-1} and z_k.

The FSDT of a laminated plate is based on the following well-known assumptions on both the strain and the stress fields:

1. the through-the-thickness transverse stress is nil, i.e. $\sigma_{33} = 0$,
2. the through-the-thickness shear stresses $\sigma_{\alpha 3}$ are continuous piecewise quadratic functions of the z coordinate,
3. straight lines perpendicular to the midplane cannot be stretched, i.e. $\varepsilon_{33} = 0$,
4. straight lines perpendicular to the midplane remain straight after deformation, i.e. $\varepsilon_{\alpha 3,3} = 0$.

From now on, Greek indices assume values $1, 2$, while Latin indices assume values $1, 2, 3$. Furthermore, the subscript comma indicates the partial derivative $f_{,j} = \partial f / \partial x_j$ and repeated indices are understood to be summed within their range, unless explicitly stated.

It is interesting to recall that the simultaneous presence of Assumptions 1 and 3 could appear to be formally incorrect. However, as proved in Ref. [19], they are consistent in a general 3D formulation of the elastic problem and they can be rationally introduced using the concepts of constrained continua.

Kinematics: The kinematical Assumptions 3. and 4. lead to the classical representation form of the displacement field:

$$\begin{aligned} s_1(x_1, x_2, z) &= u_1(x_1, x_2) + z\varphi_1(x_1, x_2), \\ s_2(x_1, x_2, z) &= u_2(x_1, x_2) + z\varphi_2(x_1, x_2), \\ s_3(x_1, x_2, z) &= w(x_1, x_2). \end{aligned} \tag{2}$$

Thus, the strain tensor can be decomposed as:

$$\varepsilon_{ij} = e_{ij} + z\kappa_{ij} + \gamma_{ij}, \tag{3}$$

where e_{ij} is the in-plane deformation, κ_{ij} the curvature and γ_{ij} the transverse shear strain:

$$\left[e_{ij}\right] = \begin{bmatrix} u_{1,1} & (u_{1,2} + u_{2,1})/2 & 0 \\ (u_{1,2} + u_{2,1})/2 & u_{2,2} & 0 \\ 0 & 0 & 0 \end{bmatrix}, \tag{4}$$

$$\left[\kappa_{ij}\right] = \begin{bmatrix} \varphi_{1,1} & (\varphi_{1,2} + \varphi_{2,1})/2 & 0 \\ (\varphi_{1,2} + \varphi_{2,1})/2 & \varphi_{2,2} & 0 \\ 0 & 0 & 0 \end{bmatrix}, \tag{5}$$

$$\left[\gamma_{ij}\right] = \begin{bmatrix} 0 & 0 & (w_{,1} + \varphi_1)/2 \\ 0 & 0 & (w_{,2} + \varphi_2)/2 \\ (w_{,1} + \varphi_1)/2 & (w_{,2} + \varphi_2)/2 & 0 \end{bmatrix}. \tag{6}$$

Constitutive equations: In a 3D framework, the constitutive relation for an orthotropic material, with two material axes arbitrarily oriented in the x_1–x_2 plane, is:

$$\sigma_{ij} = \mathscr{C}_{ijhk}\varepsilon_{hk} \quad \text{or} \quad \varepsilon_{ij} = \mathscr{S}_{ijhk}\sigma_{hk}, \tag{7}$$

where $\mathscr{C}$ is the fourth-order elasticity matrix, and $\mathscr{S} = \mathscr{C}^{-1}$ the compliance matrix. Because of the orthotropy $\mathscr{C}_{\alpha\beta\gamma 3} = \mathscr{S}_{\alpha\beta\gamma 3} = 0$; thus, the stress–strain relations (7) can be rewritten in the form:

$$\begin{aligned} \sigma_{\alpha\beta} &= \overline{\mathscr{C}}_{\alpha\beta\gamma\delta}\left[\varepsilon_{\alpha\beta} - \mathscr{S}_{\gamma\delta 33}\sigma_{33}\right], \\ \varepsilon_{\alpha 3} &= 2\mathscr{S}_{\alpha 3\gamma 3}\sigma_{\gamma 3}, \\ \varepsilon_{33} &= \mathscr{S}_{33\gamma\delta}\sigma_{\gamma\delta} + \mathscr{S}_{3333}\sigma_{33}. \end{aligned} \tag{8}$$

Note that $\overline{\mathscr{C}} = \overline{\mathscr{S}}^{-1}$, with $\overline{\mathscr{S}}$ the reduced in-plane compliance matrix such that $\overline{\mathscr{S}}_{\alpha\beta\gamma\delta} = \mathscr{S}_{\alpha\beta\gamma\delta}$.

Taking into account the stress assumption $\sigma_{33} = 0$ and the strain decomposition (3), the in-plane stress–strain relation (first equation of Eq. (8)) for the FSDT becomes:

$$\sigma^{(k)}_{\alpha\beta} = \overline{\mathscr{C}}^{(k)}_{\alpha\beta\gamma\delta}\ \varepsilon_{\alpha\beta} = \overline{\mathscr{C}}^{(k)}_{\alpha\beta\gamma\delta}\ \left(e_{\alpha\beta} + z\ \kappa_{\alpha\beta}\right). \tag{9}$$

Through-the-thickness shear stress: An accurate evaluation for the through-the-thickness shear stress can be recovered using the 3D equilibrium equations [20,21]. For simplicity, no in-plane loads per unit volume are considered in the following; thus, it results:

$$\hat{\sigma}^{(k)}_{\alpha 3} = \hat{\sigma}^{(k)_o}_{\alpha 3} - \int_{z_{k-1}}^{z} \left(\sigma^{(k)}_{\alpha 1,1} + \sigma^{(k)}_{\alpha 2,2}\right) \mathrm{d}\zeta, \tag{10}$$

where k is the index relative to the generic laminate layer and:

$$\hat{\sigma}_{\alpha 3}^{(k)_o} = -\sum_{i=1}^{k-1} \int_{z_{i-1}}^{z_i} \left(\sigma_{\alpha 1,1}^{(i)} + \sigma_{\alpha 2,2}^{(i)} \right) \mathrm{d}\zeta, \tag{11}$$

with $\hat{\sigma}_{\alpha 3}^{(1)_o} = 0$. In other words, the shear stress profile is obtained imposing layer by layer $\sigma_{\alpha 3} = \hat{\sigma}_{\alpha 3}$, i.e. the equality between the elastic shear stress $\sigma_{\alpha 3}$ and the equilibrated shear stress $\hat{\sigma}_{\alpha 3}$ obtained from Eq. (10). Note that the stress $\sigma_{\alpha 3}$ is indicated as elastic because it accounts for the elastic deformability in the thickness of the plate, as it will be clarified in the next section.

Now, the consistency of Assumption 2 in relation to the kinematical Assumptions 3 and 4 clearly appears. In fact, substituting the in-plane constitutive equation (9) into expression (10), it is possible to compute the function $\hat{\sigma}_{\alpha 3}$ for the kth layer as:

$$\hat{\sigma}_{\alpha 3}^{(k)} = \hat{\sigma}_{\alpha 3}^{(k)_o} - \int_{z_{k-1}}^{z} \overline{\mathscr{C}}_{\alpha\beta\gamma\delta}^{(k)} \left(e_{\gamma\delta,\beta} + \zeta \ \kappa_{\gamma\delta,\beta} \right) \mathrm{d}\zeta. \tag{12}$$

Since the in-plane strains for the kinematical assumptions are linear functions of the thickness coordinate, their integrals are quadratic functions layer per layer.

3. Partial-mixed principle for FSDT

This section introduces a partial-mixed variational principle for laminated composite plates. The use of the proposed functional is particularly well suited for a rational deduction of the FSDT governing equations, for the definition of refined FSDT models and also for the development of a robust finite element. The functional is named partial-mixed since both the displacements u_1, u_2, w, φ_1, φ_2 and the shear stresses $\sigma_{\alpha 3}$ are considered as independent fields.

For the 3D body Ω subjected to body forces b_i, tractions p_i on $\partial_f\Omega$ and assigned displacements $\hat{s}_i$ on $\partial_s\Omega$, the Hellinger–Reissner mixed functional is:

$$\begin{aligned} R(s_i, \sigma_{ij}) = & -\frac{1}{2} \int_\Omega \sigma_{ij} \mathscr{S}_{ijhk} \sigma_{hk} \, \mathrm{d}v + \int_\Omega \sigma_{ij} \left(s_{i,j} + s_{j,i} \right)/2 \, \mathrm{d}v \\ & \int_\Omega b_i s_i \, \mathrm{d}v - \int_{\partial_f\Omega} p_i s_i \, \mathrm{d}a \\ & - \int_{\partial_s\Omega} \sigma_{ij} n_j \left(s_i - \hat{s}_i \right) \mathrm{d}a. \end{aligned} \tag{13}$$

Substitution of relations (8) into Eq. (13) returns a partial-mixed functional:

$$\begin{aligned} \overline{\Pi}(s_i, \sigma_{\alpha 3}, \sigma_{33}) = & \ \overline{\Pi}^{\mathrm{s}}(s_\alpha, s_3, \sigma_{\alpha 3}) \\ & + \frac{1}{2} \int_\Omega \overline{\mathscr{C}}_{\alpha\beta\gamma\delta} \left(s_{\gamma,\delta} + s_{\delta,\gamma} \right)/2 \\ & \left(s_{\alpha,\beta} + s_{\beta,\alpha} \right)/2 \, \mathrm{d}v \\ & - \int_\Omega \overline{\mathscr{C}}_{\alpha\beta\gamma\delta} \mathscr{S}_{\gamma\delta 33} \sigma_{33} \left(s_{\alpha,\beta} + s_{\beta,\alpha} \right)/2 \\ & + \int_\Omega \sigma_{33} s_{3,3} \, \mathrm{d}v \\ & - \frac{1}{2} \int_\Omega \left(\mathscr{S}_{3333} - \mathscr{S}_{33\alpha\beta} \overline{\mathscr{C}}_{\alpha\beta\gamma\delta} \mathscr{S}_{\gamma\delta 33} \right) \sigma_{33}^2 \, \mathrm{d}v \\ & - \int_\Omega b_i s_i \, \mathrm{d}v - \int_{\partial_f\Omega} p_i s_i \, \mathrm{d}a \\ & - \int_{\partial_s\Omega} \sigma_{33} n_3 \left(s_3 - \hat{s}_3 \right) \mathrm{d}a \\ & - \int_{\partial_s\Omega} \overline{\mathscr{C}}_{\alpha\beta\gamma\delta} \left[\left(s_{\gamma,\delta} + s_{\delta,\gamma} \right)/2 \right. \\ & \left. - \mathscr{S}_{\gamma\delta 33} \sigma_{33} \right] n_\beta \left(s_\alpha - \hat{s}_\alpha \right) \mathrm{d}a \\ & - \int_{\partial_s\Omega} \sigma_{\alpha 3} n_3 \left(s_\alpha - \hat{s}_\alpha \right) \mathrm{d}a \\ & - \int_{\partial_s\Omega} \sigma_{3\alpha} n_\alpha \left(s_3 - \hat{s}_3 \right) \mathrm{d}a, \end{aligned} \tag{14}$$

where $\overline{\Pi}^{\mathrm{s}}$ accounts for the transverse shear deformation:

$$\overline{\Pi}^{\mathrm{s}}(s_i, \sigma_{\alpha 3}) = -\frac{1}{2} \int_\Omega 4 \mathscr{S}_{\alpha 3 \gamma 3} \sigma_{\gamma 3} \sigma_{\alpha 3} \, \mathrm{d}v + \int_\Omega \sigma_{\alpha 3} (s_{3,\alpha} + s_{\alpha,3}) \, \mathrm{d}v. \tag{15}$$

To specialize functional (14) to the case of FSDT laminates, the assumptions on the normal and the shear stresses in the thickness direction as well as the representation form of the displacement are introduced. Then, integration through the thickness returns the partial-mixed functional relative to the laminate:

$$\Pi(u_\alpha, w, \varphi_\alpha, \sigma_{\alpha 3}) = \Pi^{\mathrm{b}}(u_\alpha, \varphi_\alpha) + \Pi^{\mathrm{s}}(w, \varphi_\alpha, \sigma_{\alpha 3}) - \Pi_{\mathrm{ext}}, \tag{16}$$

where Π_{ext} accounts for the loading and the boundary conditions, Π^{b} contains the bending and the extensional terms:

$$\Pi^{\mathrm{b}}(u_\alpha,\varphi_\alpha)=\frac{1}{2}\int_A \mathscr{A}_{\alpha\beta\gamma\delta}\big(u_{\gamma,\delta}+u_{\delta,\gamma}\big)/2\big(u_{\alpha,\beta}+u_{\beta,\alpha}\big)/2\,\mathrm{d}A + \int_A \mathscr{B}_{\alpha\beta\gamma\delta}\big(\varphi_{\gamma,\delta}+\varphi_{\delta,\gamma}\big)/2\big(u_{\alpha,\beta}+u_{\beta,\alpha}\big)/2\,\mathrm{d}A + \frac{1}{2}\int_A \mathscr{D}_{\alpha\beta\gamma\delta}\big(\varphi_{\gamma,\delta}+\varphi_{\delta,\gamma}\big)/2\big(\varphi_{\alpha,\beta}+\varphi_{\beta,\alpha}\big)/2\,\mathrm{d}A, \tag{17}$$

while Π^{s} contains the transverse shear terms:

$$\Pi^{\mathrm{s}}(w,\varphi_\alpha,\sigma_{\alpha3}) = -\frac{1}{2}\int_\Omega 4\mathscr{S}_{\alpha3\gamma3}\sigma_{\gamma3}\sigma_{\alpha3}\,\mathrm{d}v + \int_A\left[(w_{,\alpha}+\varphi_\alpha)\int_{-h}^{h}\sigma_{\alpha3}\,\mathrm{d}z\right]\mathrm{d}A. \tag{18}$$

The fourth-order in-plane, coupling and bending elasticity matrices are respectively given by:

$$\mathscr{A}_{\alpha\beta\gamma\delta}=\sum_{k=1}^{n}(z_k-z_{k-1})\overline{\mathscr{C}}^{(k)}_{\alpha\beta\gamma\delta},$$
$$\mathscr{B}_{\alpha\beta\gamma\delta}=\frac{1}{2}\sum_{k=1}^{n}(z_k^2-z_{k-1}^2)\overline{\mathscr{C}}^{(k)}_{\alpha\beta\gamma\delta}, \tag{19}$$
$$\mathscr{D}_{\alpha\beta\gamma\delta}=\frac{1}{3}\sum_{k=1}^{n}(z_k^3-z_{k-1}^3)\overline{\mathscr{C}}^{(k)}_{\alpha\beta\gamma\delta}.$$

Moreover, in Eq. (18) the quantity:

$$\int_{-h}^{h}\sigma_{\alpha3}\,\mathrm{d}z=Q_\alpha \tag{20}$$

represents the resultant shear stress in the laminate.

The stationary conditions of Π with respect to the parameters $u_\alpha, w, \varphi_\alpha, \sigma_{\alpha3}$ lead to the field and the boundary laminate governing equations. Next, for the sake of simplicity, only the field equations are reported. In particular, the stationary condition of Π with respect to u_α returns the in-plane equilibrium equation:

$$\int_A\big[\mathscr{A}_{\alpha\beta\gamma\delta}\big(u_{\gamma,\delta}+u_{\delta,\gamma}\big)/2 + \mathscr{B}_{\alpha\beta\gamma\delta}\big(\varphi_{\gamma,\delta}+\varphi_{\delta,\gamma}\big)/2\big]\,\delta u_{\alpha,\beta}\,\mathrm{d}A=0. \tag{21}$$

Similarly, the stationary condition with respect to w returns the transverse equilibrium equation:

$$\int_A(Q_\alpha\,\delta w_{,\alpha}-q_3\,\delta w)\,\mathrm{d}A=0, \tag{22}$$

where q_3 is the transverse distributed load. The stationary condition with respect to φ_α returns the rotational equilibrium equation:

$$\int_A\big\{\big[\mathscr{B}_{\alpha\beta\gamma\delta}\big(u_{\gamma,\delta}+u_{\delta,\gamma}\big)/2+\mathscr{D}_{\alpha\beta\gamma\delta}\big(\varphi_{\gamma,\delta}+\varphi_{\delta,\gamma}\big)/2\big]\,\delta\varphi_{\alpha,\beta} + Q_\alpha\,\delta\varphi_\alpha\big\}\,\mathrm{d}A=0. \tag{23}$$

The stationary condition with respect to $\sigma_{\alpha3}$ leads to the constitutive equation:

$$\int_A\left\{\int_{-h}^{h}\big[(w_{,\alpha}+\varphi_\alpha)-4\mathscr{S}_{\alpha3\gamma3}\sigma_{\gamma3}\big]\,\delta\sigma_{\alpha3}\,\mathrm{d}z\right\}\mathrm{d}A=0. \tag{24}$$

Of course, boundary conditions are associated to each of Eqs. (21)–(24).

Now, different laminate models can be deduced through different choices of the shear stress profile $\sigma_{\alpha3}$ in the partial-mixed functional (16), i.e. in Eqs. (20) and (24) [1]. In particular, two different FSDT refined laminate models are proposed. The models are named refined since, accordingly to Assumption 2, they account for the consistent piecewise quadratic shear stresses in the laminate thickness.

Remark: At this stage, the shear stress profile can be explicitly derived by the equilibrium equation (10) for special cases. As an example, for a homogeneous orthotropic plate, the coupling matrix $\mathscr{B}_{\alpha\beta\gamma\delta}$ is nil, hence the equilibrium equations (21) and (23) decouple in independent in-plane and bending equations. In particular, from Eq. (21) it results $e_{\gamma\delta,\beta}=0$, then formula (12) gives:

$$\hat{\sigma}_{\alpha3}=-\int_{-h}^{z}\zeta\overline{\mathscr{C}}_{\alpha\beta\gamma\delta}\kappa_{\gamma\delta,\beta}\,\mathrm{d}\zeta=\frac{1}{2}\big(h^2-z^2\big)\overline{\mathscr{C}}_{\alpha\beta\gamma\delta}\kappa_{\gamma\delta,\beta} \tag{25}$$

and the resultant shear stress (20) becomes:

$$Q_\alpha=\frac{1}{2}\overline{\mathscr{C}}_{\alpha\beta\gamma\delta}\kappa_{\gamma\delta,\beta}\int_{-h}^{h}\big(h^2-z^2\big)\,\mathrm{d}z=\frac{1}{2}\,\overline{\mathscr{C}}_{\alpha\beta\gamma\delta}\kappa_{\gamma\delta,\beta}\frac{4}{3}h^3. \tag{26}$$

Combining Eqs. (25) and (26), the shear stress profile is recovered as:

$$\hat{\sigma}_{\alpha3}=\frac{3}{4h^3}\big(h^2-z^2\big)Q_\alpha, \tag{27}$$

which is a classical result.

For a laminate in cylindrical bending, it is $e_{22}=e_{12}=0$ and also $\kappa_{22}=\kappa_{12}=0$. Formula (12) becomes:

$$\hat{\sigma}_{13}^{(k)}=\hat{\sigma}_{13}^{(k)_o}-\int_{z_{k-1}}^{z}\Big[\overline{\mathscr{C}}^{(k)}_{1111}(e_{11,1}+\zeta\;\kappa_{11,1})\Big]\,\mathrm{d}\zeta. \tag{28}$$

On the other hand, equilibrium equations (21) and (23) take the simplified form:

[1] From the inspection of functional (18), it is clear that the stress $\sigma_{\alpha3}$ is responsible for the shear deformation in the laminate thickness, i.e. it provides the through-the-thickness shear elasticity. This is the reason because in the previous section $\sigma_{\alpha3}$ is named elastic stress.

$$0 = \mathscr{A}_{1111} e_{11,1} + \mathscr{B}_{1111} \kappa_{11,1},$$
$$Q_1 = \mathscr{B}_{1111} e_{11,1} + \mathscr{D}_{1111} \kappa_{11,1}, \tag{29}$$

whose solution is:

$$e_{11,1} = -\frac{\mathscr{B}_{1111}}{\mathscr{A}_{1111}\mathscr{D}_{1111} - \mathscr{B}_{1111}^2} Q_1,$$
$$\kappa_{11,1} = \frac{\mathscr{A}_{1111}}{\mathscr{A}_{1111}\mathscr{D}_{1111} - \mathscr{B}_{1111}^2} Q_1. \tag{30}$$

Substituting expression (30) into formula (28), the explicit piecewise quadratic form for the shear stress profile is obtained.

4. Refined FSDT: Model 1

The first refined model, named in the following as RM1-FSDT, is based on the a priori choice of suitable shear stress profiles.

In accordance with formula (12), the shear stress function $\sigma_{\alpha 3}$ can be assumed to have the form:

$$\sigma_{\alpha 3}^{(k)} = \sigma_{\alpha 3}^{(k)_o} + \overline{a}_\alpha (z+h) - \overline{\mathscr{C}}_{\alpha\beta\gamma\delta}^{(k)} \left[\overline{e}_{\gamma\delta,\beta}(z - z_{k-1}) + \frac{1}{2}\, \overline{\kappa}_{\gamma\delta,\beta}\left(z^2 - z_{k-1}^2\right) \right], \tag{31}$$

where $\overline{e}_{\gamma\delta}$ and $\overline{\kappa}_{\gamma\delta}$ are now regarded as independent shear stress parameters and no more as parameters related to the laminate kinematics. According to formula (11), the shear stress $\sigma_{\alpha 3}^{(k)_o}$ at bottom of the generic kth layer is:

$$\sigma_{\alpha 3}^{(k)_o} = \sum_{i=1}^{k-1} \overline{a}_\alpha (z_i + h) - \overline{\mathscr{C}}_{\alpha\beta\gamma\delta}^{(i)} \left[\overline{e}_{\gamma\delta,\beta}(z_i - z_{i-1}) + \frac{1}{2}\, \overline{\kappa}_{\gamma\delta,\beta}\left(z_i^2 - z_{i-1}^2\right) \right]. \tag{32}$$

Moreover, the quantity $\overline{a}_\alpha$ is set such that $\overline{\sigma}_{\alpha 3} = 0$ on the top of the laminate, i.e.:

$$\overline{a}_\alpha = \frac{\sum_{i=1}^n \overline{\mathscr{C}}_{\alpha\beta\gamma\delta}^{(i)} \left[\overline{e}_{\gamma\delta,\beta}(z_i - z_{i-1}) + \frac{1}{2}\, \overline{\kappa}_{\gamma\delta,\beta}\left(z_i^2 - z_{i-1}^2\right) \right]}{\sum_{i=1}^n (z_i + h)}. \tag{33}$$

Hence, the $\sigma_{\alpha 3}^{(k)}$ is function only of the new independent parameters $\overline{e}_{\gamma\delta}$ and $\overline{\kappa}_{\gamma\delta}$.

The equation governing the RM1-FSDT are obtained substituting the representation form (31) into the variational equations (21)–(24). In particular, Eqs. (21)–(23) remain unchanged, and the resultant shear stress (20) is:

$$\begin{aligned} Q_\alpha &= \sum_{k=1}^n \int_{z_{k.1}}^{z_k} \left\{ \sigma_{\alpha 3}^{(k)_o} + \overline{a}_\alpha (z+h) - \overline{\mathscr{C}}_{\alpha\beta\gamma\delta}^{(k)} \left[\overline{e}_{\gamma\delta,\beta}(z - z_{k-1}) + \frac{1}{2}\, \overline{\kappa}_{\gamma\delta,\beta}\left(z^2 - z_{k-1}^2\right) \right] \right\} \mathrm{d}z \\ &= \sum_{k=1}^n \left\{ \sigma_{\alpha 3}^{(k)_o} \phi_0^{(k)} + \overline{a}_\alpha \phi_1^{(k)} - \overline{\mathscr{C}}_{\alpha\beta\gamma\delta}^{(k)} \left[\overline{e}_{\gamma\delta,\beta} \phi_2^{(k)} + \frac{1}{2}\, \overline{\kappa}_{\gamma\delta,\beta} \phi_3^{(k)} \right] \right\}, \end{aligned} \tag{34}$$

where:

$$\begin{aligned} \phi_0^{(k)} &= (z_k - z_{k-1}), \\ \phi_1^{(k)} &= \frac{1}{2}(z_k - z_{k-1})(z_{k-1} + z_k + 2h), \\ \phi_2^{(k)} &= \frac{1}{2}(z_k - z_{k-1})^2, \\ \phi_3^{(k)} &= \frac{1}{3}(z_k - z_{k-1})^2 (2 z_{k-1} + z_k). \end{aligned} \tag{35}$$

Furthermore, taking into account position (31), Eq. (24) becomes:

$$\begin{aligned} 0 = \int_A \sum_{k=1}^n \int_{z_{k.1}}^{z_k} \Bigg\{ & (w_{,\alpha} + \varphi_\alpha) \Bigg[\phi_0^{(k)}\, \delta\sigma_{\alpha 3}^{(k)_o} + \phi_1^{(k)}\, \delta\overline{a}_\alpha \\ & - \overline{\mathscr{C}}_{\alpha\beta\lambda\mu}^{(k)} \left(\phi_2^{(k)}\, \delta\overline{e}_{\lambda\mu,\beta} + \frac{1}{2} \phi_3^{(k)}\, \delta\overline{\kappa}_{\lambda\mu,\beta} \right) \Bigg] \\ & - 4\mathscr{S}_{\alpha 3\gamma 3}^{(k)} \Bigg[\sigma_{\gamma 3}^{(k)_o} \phi_0^{(k)} + \overline{a}_\gamma \phi_1^{(k)} \\ & - \overline{\mathscr{C}}_{\gamma\delta\eta\theta}^{(k)} \left(\overline{e}_{\eta\theta,\delta} \phi_2^{(k)} + \frac{1}{2} \overline{\kappa}_{\eta\theta,\delta} \phi_3^{(k)} \right) \Bigg] \delta\sigma_{\alpha 3}^{(k)_o} \\ & - 4\mathscr{S}_{\alpha 3\gamma 3}^{(k)} \Bigg[\sigma_{\gamma 3}^{(k)_o} \phi_1^{(k)} + \overline{a}_\gamma \phi_{11}^{(k)} \\ & - \overline{\mathscr{C}}_{\gamma\delta\eta\theta}^{(k)} \left(\overline{e}_{\eta\theta,\delta} \phi_{12}^{(k)} + \frac{1}{2} \overline{\kappa}_{\eta\theta,\delta} \phi_{13}^{(k)} \right) \Bigg] \delta\overline{a}_\alpha \\ & + 4\mathscr{S}_{\alpha 3\gamma 3}^{(k)} \Bigg[\sigma_{\gamma 3}^{(k)_o} \phi_2^{(k)} + \overline{a}_\gamma \phi_{12}^{(k)} \\ & - \overline{\mathscr{C}}_{\gamma\delta\eta\theta}^{(k)} \left(\overline{e}_{\eta\theta,\delta} \phi_{22}^{(k)} + \frac{1}{2} \overline{\kappa}_{\eta\theta,\delta} \phi_{23}^{(k)} \right) \Bigg] \overline{\mathscr{C}}_{\alpha\beta\lambda\mu}^{(k)}\, \delta\overline{e}_{\lambda\mu,\beta} \\ & + 2\mathscr{S}_{\alpha 3\gamma 3}^{(k)} \Bigg[\sigma_{\gamma 3}^{(k)_o} \phi_3^{(k)} + \overline{a}_\gamma \phi_{13}^{(k)} \\ & - \overline{\mathscr{C}}_{\gamma\delta\eta\theta}^{(k)} \left(\overline{e}_{\eta\theta,\delta} \phi_{23}^{(k)} + \frac{1}{2} \overline{\kappa}_{\eta\theta,\delta} \phi_{33}^{(k)} \right) \Bigg] \\ & \overline{\mathscr{C}}_{\alpha\beta\lambda\mu}^{(k)}\, \delta\overline{\kappa}_{\lambda\mu,\beta} \Bigg\} \mathrm{d}z\, \mathrm{d}A, \end{aligned} \tag{36}$$

where:

$$\phi_{11}^{(k)} = \frac{1}{3}(z_k - z_{k-1})\big(z_{k-1}^2 + 3h^2 + (3h + z_k)(z_{k-1} + z_k)\big),$$
$$\phi_{12}^{(k)} = \frac{1}{6}(z_k - z_{k-1})^2(z_{k-1} + 2z_k + 3h),$$
$$\phi_{13}^{(k)} = \frac{1}{12}(z_k - z_{k-1})^2\left(z_{k-1}^2 + (8h + 6z_k)\left(z_{k-1} + \frac{1}{2}z_k\right)\right),$$
$$\phi_{22}^{(k)} = \frac{1}{3}(z_k - z_{k-1})^3,$$
$$\phi_{23}^{(k)} = \frac{1}{12}(z_k - z_{k-1})^3(5z_{k-1} + 3z_k),$$
$$\phi_{33}^{(k)} = \frac{1}{12}(z_k - z_{k-1})^3\big(8z_{k-1}^2 + 9z_k z_{k-1} + 3z_k^2\big). \tag{37}$$

Finally, due to Eqs. (32) and (33), it results:

$$\delta\overline{a}_\alpha = \frac{\sum_{i=1}^n \overline{\mathscr{C}}\alpha\beta\gamma\delta^{(i)}(z_i - z_{i-1})}{\sum_{i=1}^n (z_i + h)}\,\delta\overline{e}_{\gamma\delta,\beta} + \frac{1}{2}\frac{\sum_{i=1}^n \overline{\mathscr{C}}^{(i)}_{\alpha\beta\gamma\delta}\big(z_i^2 - z_{i-1}^2\big)}{\sum_{i=1}^n (z_i + h)}\,\delta\overline{\kappa}_{\gamma\delta,\beta}, \tag{38}$$

$$\delta\sigma_{\alpha3}^{(k)_o} = \sum_{j=1}^{k-1}\left[\big(z_j + h\big)\frac{\sum_{i=1}^n \overline{\mathscr{C}}^{(i)}_{\alpha\beta\gamma\delta}(z_i - z_{i-1})}{\sum_{i=1}^n (z_i + h)} - \overline{\mathscr{C}}^{(j)}_{\alpha\beta\gamma\delta}\big(z_j - z_{i-1}\big)\right]\delta\overline{e}_{\gamma\delta,\beta} + \sum_{j=1}^{k-1}\frac{1}{2}\left[\big(z_j + h\big)\frac{\sum_{i=1}^n \overline{\mathscr{C}}^{(i)}_{\alpha\beta\gamma\delta}\big(z_i^2 - z_{i-1}^2\big)}{\sum_{i=1}^n (z_i + h)} - \frac{1}{2}\overline{\mathscr{C}}^{(j)}_{\alpha\beta\gamma\delta}\Big(z_j^2 - z_{j-1}^2\Big)\right]\delta\overline{\kappa}_{\gamma\delta,\beta}. \tag{39}$$

Thus, Eq. (36) leads to the definition of 6 equations which are added to the 5 equilibrium equations (21), (22) and (23). In conclusion, the RM1-FSDT is defined by 11 global unknown parameters: 5 kinematical parameters plus 6 shear stress parameters.

The high number of unknowns does not represent a strong drawback of the RM1-FSDT. In fact, the 6 added parameters are not kinematical quantities, and thus, in a finite element implementation, they can be condensed at element level, leading to the classical 5 d.o.f. per node element.

5. Refined FSDT: Model 2

The second refined FSDT model, named in the following as RM2-FSDT, is based on a procedure solving iteratively two simpler sub-problems: the computation of the laminate response and the determination of the shear stress profile through the 3D equilibrium equations. The procedure is rationally derived from the partial-mixed functional (16), and recover the analytical approach proposed by Noor and coworkers in Refs. [16–18] for the case of rectangular laminates subjected to sinusoidal loading. Furthermore, the procedure is implemented into a finite element scheme.

5.1. Governing equations

Let the through-the-thickness shear stress shape function g_α be introduced as:

$$g_\alpha(x_1, x_2, z) = \frac{\sigma_{\alpha3}(x_1, x_2, z)}{Q_\alpha(x_1, x_2)} \;\Rightarrow\; \sigma_{\alpha3} = g_\alpha\, Q_\alpha \quad (\text{no sum on } \alpha). \tag{40}$$

Because of Assumption 2, g_α is a continuous piecewise quadratic function of the z coordinate with:

$$g_\alpha(x_1, x_2, -h) = g_\alpha(x_1, x_2, h) = 0 \quad \forall (x_1, x_2) \in \mathscr{A} \tag{41}$$

and

$$\int_{-h}^{h}\sigma_{\alpha3}\,\mathrm{d}z = \int_{-h}^{h} g_\alpha\, Q_\alpha\,\mathrm{d}z = Q_\alpha \;\Rightarrow\; \int_{-h}^{h} g_\alpha\,\mathrm{d}z = 1. \tag{42}$$

Note that, the function g_α is in general not constant in the in-plane coordinates.

For the homogeneous plate, in accordance with expression (27), the shape function g_α can be assigned a priori as:

$$g_\alpha = \frac{3}{4h^3}\big(h^2 - z^2\big), \tag{43}$$

while, as emphasized in the introduction, for composite laminates it is not possible to assign g_α a priori.

Taking into account position (40), Eq. (24) takes the form:

$$\begin{aligned} 0 &= \int_A\left\{\int_{-h}^{h}\big[(w_{,\alpha} + \varphi_\alpha) - 4\mathscr{S}_{\alpha3\gamma3}\; g_\gamma Q_\gamma\big]\delta(g_\alpha Q_\alpha)\,\mathrm{d}z\right\}\mathrm{d}A \\ &= \int_A\left\{\left[(w_{,\alpha} + \varphi_\alpha) - Q_\gamma\int_{-h}^{h} 4\mathscr{S}_{\alpha3\gamma3}\; g_\alpha g_\gamma\,\mathrm{d}z\right]\delta Q_\alpha\right\}\mathrm{d}A \\ &\quad + \int_A\left\{\int_{-h}^{h}\big[(w_{,\alpha} + \varphi_\alpha) - 4\mathscr{S}_{\alpha3\gamma3} g_\gamma Q_\gamma\big] Q_\alpha\,\delta g_\alpha\,\mathrm{d}z\right\}\mathrm{d}A. \end{aligned} \tag{44}$$

Contrary to the classical FSDT, herein the shape function g_α represents an unknown of the problem. As previously emphasized, the laminate problem is now spited into two sub-problems.

Laminate response: The determination of the laminate response is obtained using a given shear stress profile, i.e. g_α is assigned, hence $\delta g_\alpha = 0$. Thus, the strong form of Eq. (44) reduces to:

$$(w_{,\alpha} + \varphi_\alpha) - \tilde{H}_{\alpha\gamma}\; Q_\gamma = 0 \;\Rightarrow\; Q_\alpha = \tilde{K}_{\alpha\gamma}\big(w_{,\gamma} + \varphi_\gamma\big), \tag{45}$$

where $\tilde{H}_{\alpha\gamma}$ is the resultant overall shear compliance matrix:

$$\tilde{H}_{\alpha\gamma} = \sum_{k=1}^{n} 4\mathscr{S}^{(k)}_{\alpha 3\gamma 3} \int_{z_{k-1}}^{z_k} g_\alpha \; g_\gamma \quad \text{(no sum)} \tag{46}$$

and $\tilde{\mathbf{K}} = \tilde{\mathbf{H}}^{-1}$. Note that the overall shear compliance matrix can be written as:

$$\tilde{H}_{\alpha\gamma} = \chi_{\alpha\gamma} \; H_{\alpha\gamma} \quad \text{(no sum)}, \tag{47}$$

where the quantities $\chi_{\alpha\gamma}$ can be interpreted as shear correction factors and:

$$H_{\alpha\gamma} = \sum_{k=1}^{n} (z_k - z_{k-1}) 4\mathscr{S}^{(k)}_{\alpha 3\gamma 3}. \tag{48}$$

Taking into account expressions (40) and (46), the shear factors are evaluated in explicit form as:

$$\chi_{\alpha\gamma} = \frac{1}{H_{\alpha\gamma}} \sum_{k=1}^{n} 4\mathscr{S}^{(k)}_{\alpha 3\gamma 3} \int_{z_{k-1}}^{z_k} g^{(k)}_\alpha \; g^{(k)}_\gamma \quad \text{(no sum)}. \tag{49}$$

In conclusion, the laminate response is governed by the equilibrium equations (21), (22) and (23) and by the averaged constitutive equation (45). If desired, the displacement formulation of the laminate problem can be obtained introducing the expression for Q_α from Eq. (45) into functional (16):

$$\begin{aligned} \Phi(u^o_\alpha, w, \varphi_\alpha) = {} & \Pi^b(u_\alpha, \varphi_\alpha) \\ & + \frac{1}{2} \int_A \tilde{K}_{\alpha\gamma} \big(w_{,\alpha} + \varphi_\gamma\big)\big(w_{,\alpha} + \varphi_\alpha\big) \, \mathrm{d}v \\ & - \Pi_{\text{ext}}. \end{aligned} \tag{50}$$

It is interesting to observe that the form of functional (50) resembles the one associated to the classical FSDT. However, in the present approach the shear matrix $\tilde{K}_{\alpha\gamma}$ is the inverse of $\tilde{H}_{\alpha\gamma}$ defined in Eq. (46), while in classical FSDT the shear matrix $\tilde{K}_{\alpha\gamma}$ is substituted with a matrix $\hat{K}_{\alpha\gamma}$ computed as:

$$\hat{K}_{\alpha\gamma} = \mu_{\alpha\gamma} \sum_{k=1}^{n} (z_k - z_{k-1}) 4\overline{\mathscr{C}}^{(k)}_{\alpha 3\gamma 3}, \tag{51}$$

where $\mu_{\alpha\gamma}$ is the classical shear factors [11]. It must be emphasized that $\chi_{\alpha\gamma}$ differs form the classical definitions of the shear correction factors $\mu_{\alpha\gamma}$. As an example, for a homogeneous laminate the function g_α is given by formula (43); accordingly, the shear factors can be computed a priori as $\chi_{11} = \chi_{22} = 6/5$ and $\chi_{12} = 0$, while $\mu_{11} = \mu_{22} = 5/6$ and $\mu_{12} = 0$.

Determination of the shear stress profile: The determination of the shear stress profiles is performed at a fixed laminate solution. The shear stresses are simply recovered using the 3D equilibrium equation (10) through the plate thickness. The computed shear stress profiles are used to define new shear shape functions by formula (40).

5.2. Finite element formulation

Within the RM2-FSDT, the partial-mixed functional (16) represents a suitable basis for the development a robust laminate finite element. However, the RM2-FSDT needs an accurate determination of the shear stresses through the 3D equilibrium equation (10). In general, this cannot be accomplished by standard low-order finite elements; in fact, the use of Eq. (10) involves the computation of the second derivatives of the displacement field. Thus, an ad hoc laminate element is developed in the following.

In the framework of the incompatible mode method [22], the in-plane strains are enhanced with a field η_α, so that functional (16) takes the form [23]:

$$\begin{aligned} \Pi(u^o_\alpha, w, \varphi_\alpha, Q_\alpha, \eta_\alpha) = {} & \frac{1}{2} \int_A \mathscr{A}_{\alpha\beta\gamma\delta} \big(u_{\gamma,\delta} + u_{\delta,\gamma} + \eta_{\gamma,\delta}\big)/2 \\ & \big(u_{\alpha,\beta} + u_{\beta,\alpha} + \eta_{\alpha,\beta}\big)/2 \, \mathrm{d}v \\ & + \int_A \mathscr{B}_{\alpha\beta\gamma\delta} \big(\varphi_{\gamma,\delta} + \varphi_{\delta,\gamma} + \eta_{\gamma,\delta}\big)/2 \\ & \big(u_{\alpha,\beta} + u_{\beta,\alpha} + \eta_{\alpha,\beta}\big)/2 \, \mathrm{d}v \\ & + \frac{1}{2} \int_A \mathscr{D}_{\alpha\beta\gamma\delta} \big(\varphi_{\gamma,\delta} + \varphi_{\delta,\gamma}\big)/2 \\ & \big(\varphi_{\alpha,\beta} + \varphi_{\beta,\alpha}\big)/2 \, \mathrm{d}v \\ & - \frac{1}{2} \int_A \tilde{H}_{\alpha\gamma} \; Q_\alpha \; Q_\gamma \, \mathrm{d}v \\ & + \int_A Q_\alpha \; (w_{,\alpha} + \varphi_\alpha) \, \mathrm{d}v \\ & - \Pi_{\text{ext}}, \end{aligned} \tag{52}$$

where g_α is taken as a given shape function.

An isoparametric 4-node composite plate element can be obtained considering the standard isoparametric map [24] and discretizing functional (52) as follows [25,23]:

- the in-plane displacement is bi-linear in the nodal parameters,
- the transverse displacement interpolation is bi-linear in the nodal parameters and is enriched with quadratic functions linked to the nodal rotations,
- the rotational interpolation is bi-linear in the nodal parameters and is enriched with added internal degrees of freedom associated to bubble functions,
- the shear interpolation is bi-linear and defined locally to each element,
- the enhanced strain is expressed as a function of 13 internal degree of freedom.

Introducing the above interpolation schemes in functional (52) and performing the stationary conditions for a single element, the stiffness matrix can be obtained. Since the enhanced strain, the bubble rotation and the resultant shear stress are parameters local to each element, they can be eliminated by static condensation.

Thus, an element with 5 global d.f. per node, named EML4 (Enhanced Mixed Linked 4-node) element, is obtained. A more detailed derivation of the EML4 element can be found in Ref. [23].

It is very important to note that the adopted mixed formulation introduces the resultant stress Q_α as a primary variable. As a consequence, an accurate evaluation of Q_α is expected.

Shear stress profile: Although the EML4 finite element is enhanced with incompatible deformation modes, the direct use of the equilibrium equation (10) do not allow a satisfactory recovery of the shear stress profiles; in fact, in the finite element scheme the equilibrium equations are not locally satisfied. On the other hand, the accurate evaluation of the resultant shear Q_α leads to the possibility of properly improving the shear stress profiles, solving the following minimum problem:

$$\min\left\{\left\|\hat{\sigma}^{(k)}_{\alpha 3}+\left(\int_{z_{k-1}}^{z}\left(\sigma^{(k)}_{\alpha 1,1}+\sigma^{(k)}_{\alpha 2,2}\right)\mathrm{d}\zeta-\hat{\sigma}^{(k)_o}_{\alpha 3}\right)\right\|\right\} \tag{53}$$

subjected to the constraints:

$$\int_{-h}^{h}\hat{\sigma}_{\alpha 3}\,\mathrm{d}z-Q_\alpha=0, \tag{54}$$

$$\hat{\sigma}_{\alpha 3}\Big|_{\pm h}=0,$$

where $\|\cdot\|$ represents a given norm.

In particular, the shear stress $\hat{\sigma}_{\alpha 3}$ is computed as:

$$\hat{\sigma}^{(k)}_{\alpha 3}=b_\alpha\left[\hat{\sigma}^{(k)_o}_{\alpha 3}+a_\alpha(z+h)-\int_{z_{k-1}}^{z}\overline{\mathscr{C}}^{(k)}_{\alpha\beta\gamma\delta}\left(e_{\gamma\delta,\beta}+\zeta\kappa_{\gamma\delta,\beta}\right)\mathrm{d}\zeta\right], \tag{55}$$

where no sum on α is performed. Then, the coefficients a_α and b_α are determined enforcing condition (54) as:

$$a_\alpha=-\frac{\overline{\sigma}^{(n)}_{\alpha 3}}{hQ_\alpha}b_\alpha=Q_\alpha/\left(\overline{Q}_\alpha+\overline{\sigma}^{(n)}_{\alpha 3}h/2\right), \tag{56}$$

where:

$$\overline{\sigma}^{(n)}_{\alpha 3}=\overline{\sigma}^{(k)}_{\alpha 3}(z)_{z=h,k=n}\overline{Q}_\alpha=\int_{-h}^{h}\overline{\sigma}^{(k)}_{\alpha 3}(z)\,\mathrm{d}z, \tag{57}$$

with:

$$\overline{\sigma}^{(k)}_{\alpha 3}(z)=\hat{\sigma}^{(k)_o}_{\alpha 3}-\int_{z_{k-1}}^{z}\overline{\mathscr{C}}^{(k)}_{\alpha\beta\gamma\delta}\left(e_{\gamma\delta,\beta}+\zeta\kappa_{\gamma\delta,\beta}\right)\mathrm{d}\zeta.$$

Finally, the shear stress shape function g_α is computed substituting the expression (55) into Eq. (40).

5.3. Iterative procedure

Once the shape function g_α is computed by formula (40), shear correction factors can be determined by employing formula (49). With the new values of g_α and $\chi_{\alpha\gamma}$ a more accurate solution for the laminate problem can be derived. Accordingly, an algorithmic procedure can be developed to iteratively improve the solution of the laminate problem and evaluation of the shear factors:

1. set initial values for the shear factors (for instance, set $\chi_{11}=\chi_{22}=\chi_{12}=1$),
2. solve the plate problem,
3. compute the through-the-thickness shear stresses by Eq. (12) or Eq. (55), and the g functions by Eq. (40),
4. determine the shear factors by expression (49),
5. repeat the procedure unless the value of a residual is lower than a prefixed tolerance. [2]

6. Numerical results

Several examples are now investigated to assess the performances of the two proposed models. In particular, analytical solutions relative to the classical and the refined FSDT as well as numerical solutions from the EML4 finite element [3] are compared with analytical 3D solutions.

Computations are developed for square cross-ply laminates, with side a and different side-to-thickness ratios $\eta=h/a$. The plates are assumed to be simply supported with boundary conditions:

$$u_2=0,\ w=0,\ \varphi_2=0 \quad \text{at } x_1=0,\ x_1=a,$$
$$u_1=0,\ w=0,\ \varphi_1=0 \quad \text{at } x_2=0,\ x_2=a,$$

and subjected to a sinusoidal distributed load $q=q_0\sin(\alpha\,x_1)\sin(\alpha\,x_2)$, where $\alpha=\pi/a$.

The lamina material is assumed to be orthotropic with properties corresponding to a high modulus graphite/epoxy composite:

$$E_L/E_T=25,\quad \nu_{TT}=0.25,$$
$$G_{LT}/E_T=0.5,\quad G_{TT}/E_T=0.2.$$

In particular, both unsymmetric 0/90 and symmetric 0/90/90/0 lamination sequences are considered.

For the case under investigation, the analytical solutions for the classical FSDT are computed as discussed in Ref. [20], i.e. setting:

$$\begin{aligned}
u&=U\cos(\alpha\,x_1)\sin(\alpha\,x_2),\\
v&=V\sin(\alpha\,x_1)\cos(\alpha\,x_2),\\
w&=W\sin(\alpha\,x_1)\sin(\alpha\,x_2),\\
\varphi_1&=\Phi_1\cos(\alpha\,x_1)\sin(\alpha\,x_2),\\
\varphi_2&=\Phi_2\sin(\alpha\,x_1)\cos(\alpha\,x_2).
\end{aligned} \tag{58}$$

[2] The prefixed tolerance is taken 10^{-12}.

[3] The EML4 laminate element has been implemented into the computer code FEAP (Finite Element Analysis Program) [26].

The analytical solution for the RM1-FSDT is obtained setting the first 5 kinematical parameters as in Eq. (58) and the further 6 kinematical parameters as:

$$\begin{aligned}
\overline{e}_{11} &= E_{11}\sin(\alpha x_1)\sin(\alpha x_2),\\
\overline{\kappa}_{11} &= \Upsilon_{11}\sin(\alpha x_1)\sin(\alpha x_2),\\
\overline{e}_{22} &= E_{22}\sin(\alpha x_1)\sin(\alpha x_2),\\
\overline{\kappa}_{22} &= \Upsilon_{22}\sin(\alpha x_1)\sin(\alpha x_2),\\
\overline{e}_{12} &= E_{12}\cos(\alpha x_1)\cos(\alpha x_2),\\
\overline{\kappa}_{12} &= \Upsilon_{12}\cos(\alpha x_1)\cos(\alpha x_2).
\end{aligned} \tag{59}$$

Moreover, the analytical solution for the RM2-FSDT is computed using the formula (58) and:

$$\begin{aligned}
Q_1 &= \Gamma_1\cos(\alpha x_1)\sin(\alpha x_2),\\
Q_2 &= \Gamma_2\sin(\alpha x_1)\cos(\alpha x_2),
\end{aligned} \tag{60}$$

within the iterative algorithm for the computation of the shear factors.

The finite element analyses, relative to the ELM4 element, are performed only on a quarter of the plate (i.e. for $0 \leqslant x_1 \leqslant a/2, 0 \leqslant x_2 \leqslant a/2$), due to the double symmetry of the problem; in particular, regular meshes of 5×5 elements are used, unless explicitly stated. Finally, the solutions of the 3D problems are computed as in Pagano [27].

The different solutions of the laminate problem are denoted in the following as:

- FSDT: analytical solution for the classical FSDT with $\chi_{\alpha\beta} = 6/5$.
- RM1-FSDT: analytical solution for the RM1-FSDT.
- RM2-FSDT: analytical solution for the RM2-FSDT.
- EML4: finite element solution for the RM2-FSDT.
- 3D-AS: exact 3D solution of Pagano.

Table 1 reports the dimensionless transverse displacement $\overline{w} = 100E_T w\eta^3/q_0 a$ at the plate center, and the dimensionless horizontal displacement $\overline{u} = 100E_T u_1\eta^3/q_0 a$ at $x_1 = 0$, $x_2 = a/2$ and $z = 0$ for unsymmetric 0/90 cross-ply laminates with different side-to-thickness ratios $\eta = h/a$.

Table 2 reports the transversal displacement $\overline{w}$ at the plate center for symmetric 0/90/90/0 cross-ply laminates again with different side-to-thickness ratios $\eta = h/a$.

Figs. 1–4 show the dimensionless shear stress profiles $t_1 = \sigma_{13}/q_0$ and $t_2 = \sigma_{23}/q_0$ evaluated at $x_1 = x_2 = a/4$ for the 0/90 and the 0/90/90/0 laminates with $\eta = 0.12$. In particular, the shear stresses computed via the analytical solution of the RM1-FSDT and the ones obtained by the use of the EML4 finite element is compared to the shear stress profiles provided by the exact 3D solution. Note that, when the RM1-FSDT is adopted, the shear stresses are evaluated either (a) by Eq. (31), or (b) by the equilibrium equation (12).

The presented numerical results show the satisfactory performances of the new refined FSDT models and of the laminate element EML4. In fact, both the analytical and the numerical laminate solutions are very close to the exact 3D one, not only in terms of transverse and in-plane displacements but also in terms of shear stress profiles.

To investigate the convergence rate for the EML4 element, square laminates with $\eta = 0.10$ subjected to sinusoidal loading are studied adopting different meshes. Tables 3 and 4 report the dimensionless displacements $\overline{w}$ and $\overline{u}$, previously defined, and the dimensionless resultant shear stress $\overline{Q} = Q_1/(q_0 a)$, computed at $x_1 = x_2 = a/4$, for the 0/90 and 0/90/90/0 laminates, respectively. In particular, the FEM results are compared to the ones obtained from the analytical iterative procedure.

The numerical convergence is proved. Moreover, it can be emphasized that even coarse mesh discretizations produce accurate results, not only in terms of displacements but also in terms of resultant shear stress; the latter aspect is a peculiar characteristic of the proposed EML4 finite element and it is the basis for an accurate recovery of the shear stress profiles.

7. Concluding remarks

A partial-mixed functional for the laminate problem has been proposed in the present work. The independent variables of the formulation are the classical FSDT kinematic parameters as well as the transverse shear stresses. The explicit presence of the transverse stress in the proposed functional allowed the derivation of FSDT refined models as well as the development of finite elements.

In particular, assuming piecewise quadratic shear stress profiles, two laminate refined models has been

Table 1
Transversal and horizontal displacements $\overline{w}$ and $\overline{u}$ for a simply supported laminate 0/90 subjected to sinusoidal load: comparison between laminate and 3D solutions

	$\overline{w}$			$\overline{u}$		
η	0.08	0.10	0.12	0.08	0.10	0.12
FSDT	11.175	11.237	1.314	−0.0629	−0.0786	−0.0943
RM1-FSDT	11.170	11.230	−1.304	−0.0629	0.0786	−0.0943
RM2-FSDT	1.171	1.232	1.305	−0.0629	−0.0786	−0.0943
EML4	1.171	1.232	1.306	−0.0634	−0.0793	−0.0951
3D-AS ($z = 0$)	1.169	1.275	1.299	−0.0629	−0.0784	−0.0939

Table 2
Transversal $\overline{w}$ for a simply supported laminate 0/90/90/0 subjected to sinusoidal load: comparison between laminate and 3D solutions

	$\overline{w}(q)$		
η	0.08	0.10	0.12
FSDT	10.6181	10.7167	10.8234
RM1-FSDT	10.6364	10.7437	10.8692
RM2-FSDT	0.6363	0.7440	0.8702
EML4	0.6364	0.7447	0.8715
3D-AS ($z = 0$)	10.6328	10.7370	10.8574

derived. The first refined model (RM1-FSDT) has been based on the use of the specific shear stress profiles directly in the proposed partial-mixed variational functional. The second refined model (RM2-FSDT) has been based on the use of the equilibrated shear stress profiles within an iterative predictor–corrector procedure for the determination of the laminate response.

Furthermore, a finite element (EML4) associated to the latter model has been developed.

The numerical applications developed proved the significative influence of the use of improved shear deformation in the laminate thickness. In fact, for the investigated cases, the solutions obtained through the RM1-FSDT and the RM2-FSDT models are very close to the 3D exact solution. Furthermore, the performances of the EML4 finite element has been shown. In particular the accuracy of the calculation of the transverse shear-stresses has been emphasized.

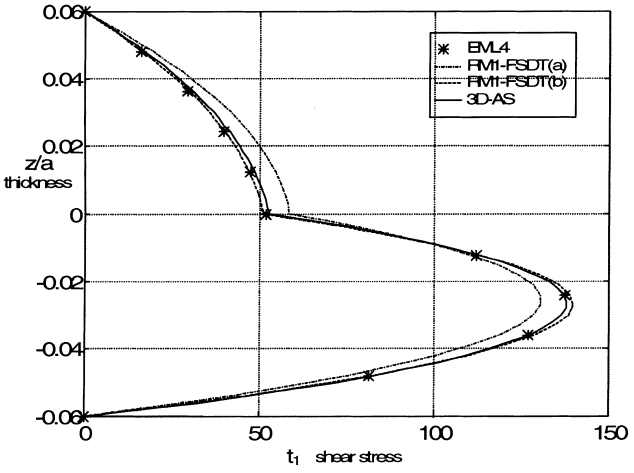

Fig. 1. Shear stress profile t_1 for a simply supported square 0/90 laminate: comparison between the RM1-FSDT, the EML4 element and the 3D analytical solution.

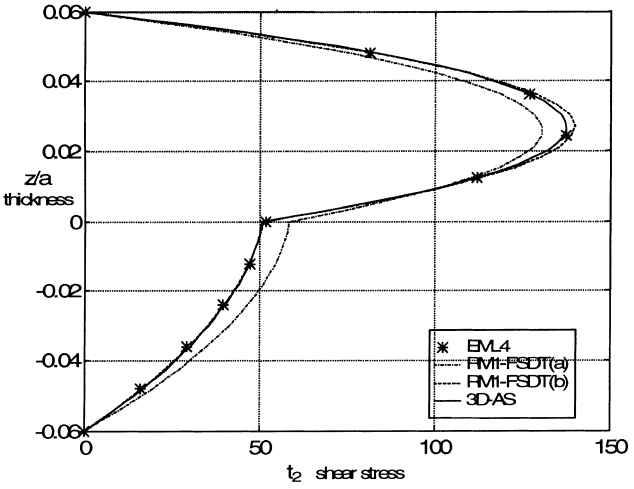

Fig. 2. Shear stress profile t_2 for a simply supported square 0/90 laminate: comparison between the RM1-FSDT, the EML4 element and the 3D analytical solution.

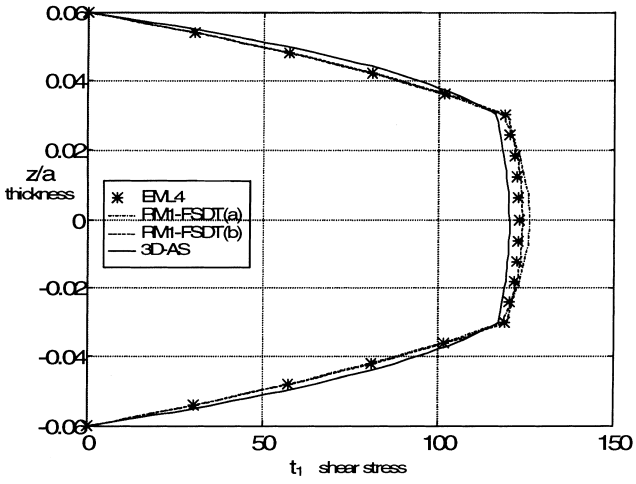

Fig. 3. Shear stress profile t_1 for a simply supported square 0/90/90/0 laminate: comparison between the RM1-FSDT, the EML4 element and the 3D analytical solution.

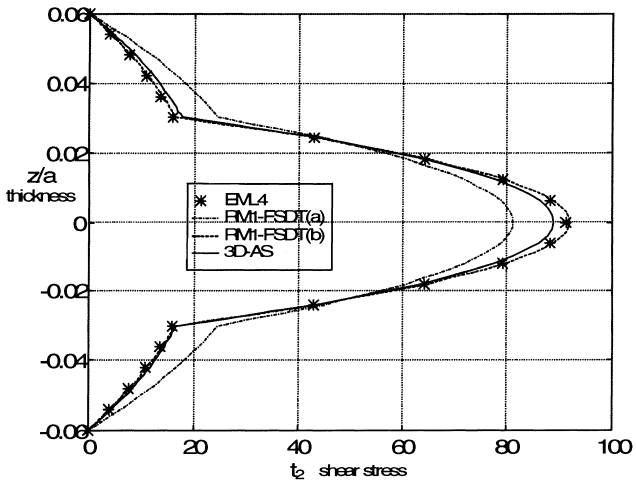

Fig. 4. Shear stress profile t_2 for a simply supported square 0/90/90/0 laminate: comparison between the RM1-FSDT, the EML4 element and the 3D analytical solution.

Table 3
Convergence of the EML4 finite element for a simply supported laminate 0/90

EML4	$\overline{w}$	$\overline{u}$	$\overline{Q}$
1×1	11.1694	−0.094443	7.2556
3×3	1.2314	−0.080466	17.7925
5×5	1.2319	−0.079279	17.8945
7×7	1.2319	−0.078955	7.9249
9×9	1.2319	−0.078822	7.9378
11×11	1.2319	−0.078755	7.9443
13×13	1.2319	−0.078716	7.9481
15×15	1.2319	−0.078692	7.9505
25×25	1.2319	−0.078646	7.9551
RM2-FSDT	1.2318	−0.078619	7.9577

Table 4
Convergence of the EML4 finite element for a simply supported laminate 0/90/90/0

EML4	$\overline{w}$	$\overline{Q}$
1×1	0.74236	10.041
3×3	0.74594	11.526
5×5	0.74472	11.680
7×7	0.74435	11.724
9×9	0.74420	11.742
11×11	0.74412	11.751
13×13	0.74408	11.756
15×15	0.74405	11.759
25×25	0.74399	11.766
RM2-FSDT	0.74402	11.766

Acknowledgements

The financial supports of the Italian National Research Council (CNR), of the Ministry of University and Research (MURST) and of the Italian Space Agency (ASI) are gratefully acknowledged.

References

[1] Reddy JN. A generalization of two-dimensional theories of laminated plates. Commun Appl Numer Meth 1987;3:173–80.
[2] Reddy JN. On refined theories of composite laminates. Meccanica 1990;25:230–38.
[3] Yang PC, Norris CH, Stavsky Y. Elastic wave propagation in heterogeneous plates. Int J Solids Struct 1966;2:665–84.
[4] Whitney JM, Pagano NJ. Shear deformation in heterogeneous anisotropic plates. J Appl Mech, Trans ASME 1970;37(92/E):1031–036.
[5] Reissner E. The effect of transverse shear deformation on the bending of elastic plates. J Appl Mech 1945;12:69–77.
[6] Mindlin RD. Influence of rotatory inertia and shear on flexural motions of isotropic, elastic plates. J Appl Mech 1951;38:31–38.
[7] Spilker RL. Hybrid-stress eight-node element for thin and thick multilayered laminated plates. Int J Numer Meth Eng 1982;18:801–28.
[8] Liou W, Sun CT. A three-dimensional hybrid stress isoparametric element for the analysis of laminated composite plates. Comp Struct 1987;25:241–49.
[9] Yong YK, Cho Y. Higher-order, partial hybrid stress, finite element formulation for laminated plate and shells analyses. Comp Struct 1995;57:817–27.
[10] Feng W. A partial hybrid degenerated plate/shell element for the analysis of laminated composites. Int J Numer Meth Eng 1996;39:3625–639.
[11] Whitney JM. Shear correction factors for orthotropic laminates under static load. J Appl Mech 1973;40:302–04.
[12] Vlachoutsis S. Shear correction factor for plates and shells. Int J Numer Meth Eng 1992;33:1537–552.
[13] Laitinen M, Lahtinen H, Sjölind SG. Transverse shear correction factors for laminates in cylindrical bending. Commun Numer Meth Eng 1995;11:41–47.
[14] Pai PF. A new look at the shear correction factors and warping functions of anisotropic laminates. Int J Solids Struct 1995;32:2295–313.
[15] Yunquin Q, Knight NF Jr. A refined first-order shear-deformation theory and its justification by plane-strain bending problem of laminated plates. Int J Solids Struct 1996;33:49–64.
[16] Noor AK, Burton WS. Stress and free vibration analyses of multilayered composite plates. Comp Struct 1989;11:183–04.
[17] Noor AK, Burton WS. Assessment of computational models for multilayered anisotropic plates. Comp Struct 1990;14:233–65.
[18] Noor AK, Burton WS, Peters JM. Predictor–corrector procedures for stress and free vibration analyses of multilayered composite plates and shells. Int J Comput Meth Appl Mech Eng 1990;82:341–63.
[19] Bisegna P, Sacco E. A rational deduction of plate theories from the three-dimensional linear elasticity. Z Angew Math Mech 1997;77:349–66.
[20] Reddy JN. Energy and variational methods in applied mechanics. New York: Wiley, 1984.
[21] Ochoa OO, Reddy JN. Finite element analysis of composite laminates. Dordrecht: Kluwer Academic Publishers, 1992.
[22] Simo JC, Rifai MS. A class of mixed assumed strain methods and the method of incompatible modes. Int J Numer Meth Eng 1990;29:1595–638.
[23] Auricchio F, Sacco E. A mixed-enhanced finite-element for the analysis of laminated composite plates. Submitted.
[24] Zienkiewicz OC, Taylor RL. The finite element method, vol. I. New York: McGraw-Hill, 1989.
[25] Auricchio F, Taylor RL. A shear deformable plate element with an exact thin limit. Int J Comput Meth Appl Mech Eng 1994;118:393–12.
[26] Manual of user of Finite Element Analysis Program. Copyright by R.L. Taylor, University of California at Berkeley. Distributed by NISEE, 1997, e-mail: nisee@ce.berkeley.edu.
[27] Pagano NJ. Exact solutions for rectangular bidirectional composites and sandwich plates. J Comp Mater 1979;4:20–34.